The rheology of Brownian suspensions

G. Bossis
Laboratoire de Physique de la Matière Condensée, Université de Nice, Parc Valrose 06034 Nice Cédex, France

J. F. Brady
Department of Chemical Engineering, California Institute of Technology, Pasadena, California 91125

(Received 15 September 1988; accepted 27 March 1989)

The viscosity of a suspension of spherical Brownian particles is determined by Stokesian dynamics as a function of the Péclet number. Several new aspects concerning the theoretical derivation of the *direct* contribution of the Brownian motion to the bulk stress are given, along with the results obtained from a simulation of a monolayer. The simulations reproduce the experimental behavior generally observed in dense suspensions, and an explanation of this behavior is given by observing the evolution of the different contributions to the viscosity with shear rate. The shear thinning at low Péclet numbers is due to the disappearance of the direct Brownian contribution to the viscosity; the deformation of the equilibrium microstructure is, however, small. By contrast, at very high Péclet numbers the suspension shear thickens due to the formation of large clusters.

I. INTRODUCTION

Predicting the rheological behavior of concentrated suspensions poses a difficult theoretical problem primarily for two reasons. First, the hydrodynamic interactions appear on several different scales. There are short-range lubrication forces between particles, which are essentially two-body contributions. There is an intermediate range in which many-body hydrodynamic interactions are important. And finally, there are also long-range, divergent, interactions that must be properly "renormalized." Second, the exact knowledge of the forces and stresses for a given configuration of the particles is not sufficient to determine the rheology, because an average over the different configurations sampled by the particles is needed. These configurations are themselves the result of the interplay between the external driving force (the imposed shear flow) and the "internal" hydrodynamic, interparticle and Brownian forces; thus, the system is completely coupled.

We have recently developed a numerical simulation method, called Stokesian dynamcis, that deals with these different aspects (cf. Ref. 1 for a review). In the case of purely hydrodynamic interactions (i.e., without interparticle forces or Brownian motion), and with configurations sampled from a Monte Carlo hard-sphere distribution, the viscosities obtained by simulation[2] as a function of the volume fraction φ, are in excellent agreement with experimental results, for example those reported by Van der Werff *et al.*[3] Furthermore, the simulations show the importance of the lubrication forces in the increase of the viscosity with increasing concentration.

In preceeding papers[4,5] we have described how to introduce Brownian motion into the evolution equation for the particle trajectories, and have discussed the changes in the suspension microstructure and the self-diffusion coefficient with increasing shear rate. In this paper we wish to focus on the rheology of Brownian suspensions and in particular, relate the change in the viscosity with shear rate to the changing microstructure. In order to save computation time we shall follow our previous studies and simulate a monolayer of identical spheres. While perhaps not directly quantitatively comparable with experiment, the resulting evolution of the viscosity with shear rate should be qualitatively accurate.

In the first part of this paper (Sec. II) we give the general relation for the various contributions to the bulk stress and offer an alternative "microscopic" derivation of the so-called *direct* contribution due to Brownian motion. In Sec. III we present the simulation results for the viscosity and the structure as a function of the Péclet number. In the discussion we compare the simulated viscosities with experiment.

II. THEORY

The calculation of the average or macroscopic stress in a homogeneous suspension has been given by Batchelor[6,7]; the deviatoric part of the stress is given by

$$\left\langle \Sigma \right\rangle = \text{I.T.} + 2\eta\langle \mathbf{E}\rangle + (1/V)\sum_{\alpha=1}^{N}\mathbf{S}_\alpha - (1/V)\sum_{\alpha=1}^{N}\mathbf{r}_\alpha\mathbf{F}_\alpha. \tag{1}$$

$\langle\Sigma\rangle$ and $\langle\mathbf{E}\rangle$ are, respectively, the macroscopic averages of the stress and rate of strain tensors defined by an integral over the volume of the suspension:

$$\langle\cdot\rangle = (1/V)\int_V d\mathbf{r}. \tag{2}$$

I.T. stands for an isotropic term of no importance for the rheology of the incompressible suspension. $\mathbf{S}_\alpha$, the stresslet exerted by the fluid on the rigid particle α located at position $\mathbf{r}_\alpha$, is the symmetric and traceless part of the first moment of the force distribution integrated over the particle surface A_α:

$$\mathbf{S}_\alpha = (1/2)\int_{A_\alpha}\{(\mathbf{r}-\mathbf{r}_\alpha)\boldsymbol{\sigma} + \boldsymbol{\sigma}(\mathbf{r}-\mathbf{r}_\alpha) - (2/3)\mathbf{I}(\mathbf{r}-\mathbf{r}_\alpha)\cdot\boldsymbol{\sigma}\}\cdot\mathbf{n}\,d\mathbf{r}. \tag{3}$$

Here $\boldsymbol{\sigma}$ is the stress tensor in the fluid, i.e., $\boldsymbol{\sigma} = -p\mathbf{I}$-

 0021-9606/89/151866-09$02.10 © 1989 American Institute of Physics

Downloaded 13 Jan 2006 to 131.215.225.172. Redistribution subject to AIP license or copyright, see http://jcp.aip.org/jcp/copyright.jsp

$+ 2\eta[\nabla\mathbf{u} + (\nabla\mathbf{u})^{\dagger}]$ with p the local fluid pressure, $\nabla\mathbf{u}$ the local fluid velocity gradient, and η is the viscosity of the suspending fluid. The normal $\mathbf{n}$ points into the fluid.

The final term in Eq. (1), $(1/V)\ \Sigma\mathbf{r}_\alpha\mathbf{F}_\alpha$, is the stress due to the interparticle forces. $\mathbf{F}_\alpha$ is the non-hydrodynamic external force exerted on particle α: the common example being the force due to an interparticle potential $V(\mathbf{r}_1,...,\mathbf{r}_N)$. (Note, a constant external force such as gravity may be included in the definition of $\mathbf{F}_\alpha$ since it does not affect the deviatoric part of the bulk stress.)

An analysis of the different components of the bulk stress has already been given, both in the context of dilute solutions[7] and in an approximate treatment of concentrated suspensions,[8] but we wish here to clarify certain points that, perhaps, appear more transparently in the context of a numerical simulation.

The local hydrodynamic stresslet of particle α is obtained with the help of the Faxén law linking the stresslet to the local rate of strain tensor $\mathbf{e}(\mathbf{r})$ evaluated at the particle's center:

$$\mathbf{S}_\alpha = (20/3)\pi\eta a^3[1 + (a^2/10)\nabla^2]\mathbf{e}|_{r=r_\alpha}. \tag{4}$$

Equation (4) is valid for spherical particles, but generalizations to nonspherical particles are possible. The local field $\mathbf{e}|_{r=r_\alpha}$ differs from the average rate of strain $\langle\mathbf{E}\rangle$ firstly because of the excluded volume due to the finite size of the particle (this is the equivalent of the well known cavity field in electrostatics), and secondly because of the nonhomogeneous (on the particle scale) repartition of the other particles around the reference particle. This difference between the local rate of strain tensor and the average one is used indirectly in the renormalization procedure of Batchelor and Green[9] and explicitly by Bedeaux[10] to obtain a Clausius–Mosotti-like formula for the viscosity.

In our approach through numerical simulation, we model an infinite suspension by periodically replicating the basic unit cell and use periodic boundary conditions. The divergent and conditionally convergent hydrodynamic interactions are renormalized by O'Brien's method,[11] and the convergence of the resulting interactions are accelerated using the Ewald summation technique.[12] This amounts to removing the $\mathbf{k} = 0$ terms in the reciprocal lattice sums.[13]

From the linearity of the governing Stokes' equations we may write the stresslets of the N particles as[1]

$$\mathbf{S} = -\mathbf{R}^*_{SU}\cdot(\mathbf{U} - \langle\mathbf{u}\rangle) + \mathbf{R}^*_{SE}:\langle\mathbf{E}\rangle - \mathbf{r}\mathbf{F}^P, \tag{5}$$

where $\mathbf{S} = (\mathbf{S}_1,\mathbf{S}_2,...,\mathbf{S}_N)$ is a column vector containing the N particle stresslets. $\mathbf{R}^*_{SU}$ and $\mathbf{R}^*_{SE}$ are part of the grand resistance matrix defined by

$$\begin{bmatrix}\mathbf{F}\\ \mathbf{S}\end{bmatrix} = -\begin{bmatrix}\mathbf{R}^*_{FU} & \mathbf{R}^*_{FE}\\ \mathbf{R}^*_{SU} & \mathbf{R}^*_{SE}\end{bmatrix}\cdot\begin{bmatrix}\mathbf{U} - \langle\mathbf{u}\rangle\\ -\langle\mathbf{E}\rangle\end{bmatrix} + \begin{bmatrix}\mathbf{F}^P\\ -\mathbf{r}\mathbf{F}^P\end{bmatrix}. \tag{6}$$

In Eq. (6) $\mathbf{U}$ stands for the translational/rotational velocities of the N particles and $\langle\mathbf{u}\rangle$ is the average velocity at the center of the particles. $\mathbf{F}$ and $\mathbf{S}$ are, respectively, the total force/torque and stresslet exerted on the N particles by the fluid *and* by the interparticle forces $\mathbf{F}^P$. The interparticle force contribution to the bulk stress given in Eq. (1) is the $-\mathbf{r}\mathbf{F}^P$ term in Eq. (6); $\mathbf{r}$ denotes the vector of particle positions. The star notation indicates that Ewald sums have been performed on the infinite periodic lattice. The resistance matrix $\mathbf{R}^*_{FU}$, etc. are purely geometric quantities, being functions of the instantaneous particle configuration only.

At low particle Reynolds numbers, the total force $\mathbf{F}$ is zero, and the particle velocities are given by

$$\mathbf{U} = \langle\mathbf{u}\rangle + \mathbf{R}^{*-1}_{FU}\cdot(\mathbf{F}^P + \mathbf{R}^*_{FE}:\langle\mathbf{E}\rangle). \tag{7}$$

The velocity in (7) does not include the contribution from Brownian motion; in the absence of an imposed flow or interparticle forces, the particles do not move. Brownian motion can be included by integrating the Langevin equation,[1,4,14] but, for our purposes in discussing the stress we only need to add a Brownian component $\mathbf{U}^B(t)$ to Eq. (7). The total stress is then obtained from the second line of Eq. (6):

$$\mathbf{S} = -(\mathbf{R}^*_{SU}\cdot\mathbf{R}^{*-1}_{FU}\cdot\mathbf{R}^*_{FE} - \mathbf{R}^*_{SE}):\langle\mathbf{E}\rangle - \mathbf{R}^*_{SU}\cdot\mathbf{U}^B - \mathbf{R}^*_{SU}\cdot\mathbf{R}^{-1}_{FU}\cdot\mathbf{F}^P - \mathbf{r}\mathbf{F}^P. \tag{8}$$

To compare with previous expressions used in the literature for the bulk stress, we write

$$\mathbf{S} = \mathbf{S}^H + \mathbf{S}^I + \mathbf{S}^B, \tag{9}$$

where

$$\mathbf{S}^H = -(\mathbf{R}^*_{SU}\cdot\mathbf{R}^{*-1}_{FU}\cdot\mathbf{R}^*_{FE} - \mathbf{R}^*_{SE}):\langle\mathbf{E}\rangle, \tag{10a}$$

$$\mathbf{S}^I = -(\mathbf{R}^*_{SU}\cdot\mathbf{R}^{*-1}_{FU} + \mathbf{r}\mathbf{I})\cdot\mathbf{F}^P, \tag{10b}$$

$$\mathbf{S}^B = -\mathbf{R}^*_{SU}\cdot\mathbf{U}^B(t). \tag{10c}$$

Here $\mathbf{I}$ is the unit isotropic tensor.

Unlike the deterministic velocity $\mathbf{U}$ in Eq. (7), the Brownian velocity $\mathbf{U}^B(t)$ fluctuates with a characteristic time equal to the Brownian relaxation time $\tau_B = m/6\pi\eta a$, which is generally several orders of magnitude smaller than the time interval Δt required for the particles to move a significant fraction (10^{-2}-10^{-3}) of their radius (or interparticle spacing). In addition to producing the Brownian displacement, these rapidly fluctuating particle velocities propagate (instantaneously in the limit of an incompressible fluid) a velocity field whose perturbations by the N particles give rise to the Brownian stress. The average of this Brownian stress over a time interval $\Delta t \gg \tau_B$ is different from zero because both $\mathbf{R}^*_{SU}$ and $\mathbf{U}^B(t)$ depend on the configuration of the particles which fluctuates at the rate of $\mathbf{U}^B(t)$. In the appendix it is shown that:

$$\mathbf{S}^B = -1/\Delta t\int_0^{\Delta t}\mathbf{R}^*_{SU}\cdot\mathbf{U}^B(t)dt = -kT\nabla\cdot(\mathbf{R}^*_{SU}\cdot\mathbf{R}^{*-1}_{FU}), \tag{11}$$

where the configuration-space divergence is with respect to the last index of $\mathbf{R}^{*-1}_{FU}$.

Owing to the symmetry of the grand resistance matrix we have

$$\mathbf{R}^*_{SU}\cdot\mathbf{R}^{*-1}_{FU} = \mathbf{R}^{*-1}_{FU}\cdot\mathbf{R}^*_{FE}, \tag{12}$$

so this quantity represents the velocity of a particle resulting from the imposed rate of strain $\langle\mathbf{E}\rangle$ [cf. Eq. (7)]. We can make a connection with the work of Batchelor[7] by noting that for two particles (α and β) alone in the fluid (i.e., pairwise hydrodynamic interactions), the components of the tensor $(\mathbf{R}^{*-1}_{FU})_{\alpha\beta}\cdot(\mathbf{R}^*_{FE})_{\alpha\beta}$ reduce to the quantity $\mathbf{C}_{\alpha\beta}$, de-

Downloaded 13 Jan 2006 to 131.215.225.172. Redistribution subject to AIP license or copyright, see http://jcp.aip.org/jcp/copyright.jsp

fined by Batchelor, giving the relative velocity of two spheres in a linear shear flow:

$$C_{jkl}(\mathbf{r}) = -(r_j r_k r_l/2r^2)(A-B) + (1/6)r_l\delta_{jk}A - (1/4)(r_j\delta_{kl} + r_k\delta_{jl})B, \quad (13)$$

where $\mathbf{r} = \mathbf{r}_\alpha - \mathbf{r}_\beta$ and A and B are functions of $|\mathbf{r}| = r$ only. The stresslet in Eq. (11) thus becomes $S_{jk} = -kT\nabla_l C_{jkl}$, which is Batchelor's result, where he used the concept of a "thermodynamic" force. Our result is, perhaps, a bit more direct, provides a microscopic definition and is not restricted to pairwise additivity. That the two definitions agree is, of course, satisfying.

Our Langevin derivation of the direct Brownian stress also serves to indicate its *hydrodynamic* origin, for it is ultimately linked to the motion of the fluid through the hydrodynamic resistance matrices. If the hydrodynamic interactions did not change with relative position or orientation of the particles, then there would be no divergence in (11) and no Brownian stress. For an isolated spherical particle, $\mathbf{R}_{SU}\cdot\mathbf{R}_{FU}^{-1}$ is a constant, namely zero, and $\mathbf{S}^B = 0$. Thus the direct Brownian stress is proportional to φ^2 for dilute concentrations of spherical particles and results from the divergence of the relative velocity [$\mathbf{C}$ in Eq. (13)] with particle separation. For nonspherical particles, however, $\mathbf{R}_{SU}\cdot\mathbf{R}_{FU}^{-1}$ is not, in general, zero for an isolated particle, and there is generally an $O(\varphi)$ direct Brownian contribution to the bulk stress. Indeed, for spheroidal particles, the orientational divergence of $\mathbf{R}_{SU}\cdot\mathbf{R}_{FU}^{-1}$ is nonzero. For an isolated spheroidal particle described by the orientation vector $\mathbf{p}$, Eq. (11) gives a contribution to the bulk stress $\langle\Sigma^B\rangle = -3\eta kT\beta\langle\mathbf{pp}\rangle$, where $\langle\mathbf{pp}\rangle$ is an orientational average and β is a function of the aspect ratio only.[15] This is precisely the result first proposed by Kirkwood and Auer[16] and Giesekus[17] and used by Hinch and Leal.[18,19] (See also Brenner[20] for a complete summary of the properties of axisymmetric particles.)

Using the above expressions for the particle stresslet, we may write the bulk stress in Eq. (1) as

$$\langle\Sigma\rangle = \text{I.T.} + 2\eta\langle\mathbf{E}\rangle + (N/V)\{\langle\mathbf{S}^H\rangle + \langle\mathbf{S}^I\rangle + \langle\mathbf{S}^B\rangle\}, \quad (14)$$

where $\langle\mathbf{S}^H\rangle = (1/N)\Sigma_{\alpha=1}{}^N\mathbf{S}_\alpha^H$ is the number average particle stresslet, and $\mathbf{S}^H$, $\mathbf{S}^I$ and $\mathbf{S}^B$ are given by Eqs. (10) and (11). Equation (14) is true for any configuration of arbitrarily shaped and sized particles. It applies instantaneously (on time scales larger than τ_B) and therefore can also be used for time-dependent flows, such as oscillatory shear or start up/cessation experiments; in this case, the impressed rate of strain $\langle\mathbf{E}\rangle$ and flow $\langle\mathbf{u}\rangle$ are now functions of time. Note also, that even in the absence of interparticle forces ($\mathbf{F}^P = 0$) and even if the magnitude of the direct Brownian stress is small, despite the appearance of Eq. (10a), the hydrodynamic stress is nonlinear in the rate of strain $\langle\mathbf{E}\rangle$ due to the fact that the particle configurations depend upon both hydrodynamic and Brownian forces. This latter dependence is the so-called *indirect* effect of Brownian motion on the stress: Brownian motion influences the structure, which in turn influences the configurational average of Eq. (10a).

Further progress can be made in the interparticle force contribution to the bulk stress if we restrict ourselves to pairwise interparticle forces. Most colloidal forces of interest are well represented by pairwise interparticle interactions, so this is not a severe restriction. Making use of Eq. (12), $\langle\mathbf{S}^I\rangle$ from Eq. (10b) becomes

$$\langle\mathbf{S}^I\rangle = -(1/N)\sum_{\alpha=1}^{N}(\mathbf{R}_{FU}^{*-1}\cdot\mathbf{R}_{FE}^{*} + \mathbf{rI})_\alpha\cdot\mathbf{F}_\alpha = -(1/N)\sum_\beta\sum_\alpha\mathbf{A}_\alpha\cdot\mathbf{F}_{\alpha\beta}. \quad (15)$$

Here, $\mathbf{A}_\alpha(\mathbf{r}_1\ldots\mathbf{r}_N) = (\mathbf{R}_{FU}^{*-1}\cdot\mathbf{R}_{FE}^{*} + \mathbf{rI})_\alpha$ is the αth component of this tensor, and when multiplied by a straining flow $\mathbf{E}$, it gives the actual velocity of particle α due to this straining flow. $\mathbf{F}_{\alpha\beta}(\mathbf{r}_\alpha - \mathbf{r}_\beta) = -\mathbf{F}_{\beta\alpha}$ is the force on particle α due to β and is only a function of the separation between α and β. Introducing the N-particle probability distribution function $P_N(\mathbf{r}_1\ldots\mathbf{r}_N)$ for N identical particles, Eq. (15) becomes without approximation

$$\langle\mathbf{S}^I\rangle = -\int\langle\mathbf{A}_1 - \mathbf{A}_2\rangle_2\cdot\mathbf{F}_{12}P_{1/1}(\mathbf{r}_2/\mathbf{r}_1)d\mathbf{r}_2, \quad (16)$$

where

$$\langle\mathbf{A}_1 - \mathbf{A}_2\rangle_2 \equiv [1/(N-2)!]\times\int(\mathbf{A}_1 - \mathbf{A}_2)P_{N-2/2}(\mathbf{r}_3\ldots\mathbf{r}_N|\mathbf{r}_1\mathbf{r}_2)d\mathbf{r}_3\ldots d\mathbf{r}_N \quad (17)$$

is the conditional average with two particles fixed at $\mathbf{r}_1$ and $\mathbf{r}_2\cdot P_{1/1}$ is the probability density for finding a particle at $\mathbf{r}_2$ given that there is a particle at $\mathbf{r}_1$.

Note in Eq. (16) that it is only through the hydrodynamic interactions that information on three particle distributions, etc. is needed. In the absence of hydrodynamic interactions, $\mathbf{A}_1 - \mathbf{A}_2 = (\mathbf{r}_1 - \mathbf{r}_2)\mathbf{I}$, and Eq. (16) depends only on pair–particle information. Under the assumption of pairwise hydrodynamic interactions, we approximate

$$\langle\mathbf{A}_1 - \mathbf{A}_2\rangle_2 = \mathbf{A}_1(\mathbf{r}_1,\mathbf{r}_2) - \mathbf{A}_2(\mathbf{r}_1,\mathbf{r}_2) = \mathbf{C}(\mathbf{r}_{12}) + \mathbf{r}_{12}\mathbf{I}, \quad (18)$$

where the last identity follows the notation of Batchelor[7] [cf. Eq. (13)]. Thus, with pairwise hydrodynamics, Eq. (16) becomes

$$\langle\mathbf{S}_{\text{PA}}^I\rangle = -\int[\mathbf{C}(\mathbf{r}_{12}) + \mathbf{r}_{12}\mathbf{I}]\cdot\mathbf{F}_{12}P_{1/2}(\mathbf{r}_2|\mathbf{r}_1)d\mathbf{r}_2, \quad (19)$$

where the subscript PA is to remind us of the pairwise hydrodynamics.

Equation (19) should be contrasted with the work of Russel and Gast[8] [their equation (31)] where they have the potential of mean force ($\nabla_{12}V_{\text{mf}} = \nabla_{12}\ln g$) rather than the actual force (or potential) between two particles ($\mathbf{F}_{12} = -\nabla_{12}V_{12}$). This difference is significant and can have an enormous impact on the values of the stress that is calculated. Our derivation here shows clearly that it is the actual two-body interparticle potential that enters into $\mathbf{S}^I$, and not the potential of mean force. The potential of mean force does, of course, play an important role in a theoretical development of the evolution equation for the pair-distribution function and possesses a good physical interpretation as a "force" in this context. But, this mean force cannot neces-

Downloaded 13 Jan 2006 to 131.215.225.172. Redistribution subject to AIP license or copyright, see http://jcp.aip.org/jcp/copyright.jsp

sarily be carried over directly as if it were a true force into the calculation of the bulk stress. Indeed, the above shows that such a carry over is incorrect.[21]

One final general point that can be made with regard to the interparticle force contribution to the bulk stress is in the case of a hard-sphere potential. A hard-sphere interparticle force is pairwise additive, so Eq. (16) applies. The hard-sphere interparticle force is only nonzero when the particles touch; $\mathbf{F}_{12} = (\mathbf{r}_{12}/|\mathbf{r}_{12}|)\ \delta(|\mathbf{r}_{12}| = 2a)$, where δ is a delta function on the surface of contact $|\mathbf{r}_{12}| = 2a$, a being the particle radius. The (x,y) component of the tensor $(\mathbf{A}_1 - \mathbf{A}_2)\cdot\mathbf{r}_{12}$ is the relative velocity of particles 1 and 2 along their line of centers due to a straining flow. This relative velocity approaches zero linearly with the surface separation, i.e., $|(\mathbf{A}_1 - \mathbf{A}_2)\cdot\mathbf{r}_{12}| \sim O(\xi)$, where $\xi = (r_{12} - 2a)/2a$, as $\xi \to 0$. This is true for any two particles and with the full many-body hydrodynamic interactions. With pairwise hydrodynamics $|(\mathbf{A}_1 - \mathbf{A}_2)\cdot\mathbf{r}_{12}| \approx 4.077\ \xi$ as $\xi \to 0$, and only the coefficient changes in going to many-body interactions, not the linear scaling with ξ. Thus, since $|\mathbf{F}_{12}| \approx O[\delta(\xi)]$, for hard spheres, the integral in Eq. (16) is proportional to $\int \xi\delta(\xi)d\xi$, which is zero. With hydrodynamic interactions the hard-sphere potential makes *no* contribution to the bulk stress. This is also the case with the particle trajectories: $\mathbf{R}_{FU}^{*-1}\cdot\mathbf{F}^P = 0$ for hard spheres in Eq. (7) because $|\mathbf{R}_{FU}^{*-1}| \sim O(\xi)$ also. With hydrodynamic interactions the hard-sphere potential has no dynamic significance. The interparticle force that appears in the particle velocity (7) and the bulk stress (10b) is an actual interparticle force of electrostatic or colloidal origin.

In our simulations to be discussed in the next section, the relative viscosity of the suspension is defined by the ratio of the xy component of the bulk stress $\langle\Sigma_{xy}\rangle$ to the xy component of the rate of strain $\langle E_{xy}\rangle$, where we are imposing a simple shear flow with $\langle u_x\rangle = \gamma y$, with γ the shear rate. Nondimensionalizing the elements of the grand resistance matrix by $6\pi\eta a$, $6\pi\eta a^2$ and $6\pi\eta a^3$, according to their respective dimensions; all lengths by the particle radius a; the time by a^2/D_0, where $D_0 = kT/6\pi\eta a$ is the diffusion coefficient of an isolated particle; the interparticle force by kT/a; and the stress by $6\pi\eta a^3\gamma$; the relative viscosity becomes

$$\eta_r = (\langle\Sigma_{xy}\rangle/2\eta\langle E_{xy}\rangle) = 1 + \eta_r^H + \eta_r^I + \eta_r^B, \tag{20}$$

with

$$\eta_r^H = (9/2)\varphi(1/N)\ \overline{\sum_{\alpha=1}^{N}(\mathbf{S}_\alpha^H)_{xy}}\ , \tag{21a}$$

$$\eta_r^I = -(9/2)\varphi(1/\mathrm{Pe})(1/N)\ \overline{\sum_{\alpha=1}^{N}(\mathbf{A}_\alpha\cdot\mathbf{F}_\alpha)_{xy}}\ , \tag{21b}$$

$$\eta_r^B = -(9/2)\varphi(1/\mathrm{Pe})(1/N)\ \overline{\sum_{\alpha=1}^{N}[\nabla_\alpha(\mathbf{R}_{FU}^{*-1}\cdot\mathbf{R}_{FE}^{*})]_{xy}}\cdot \tag{21c}$$

The over bar is to indicate a time average over the course of the dynamic simulation.

The fundamental parameters that appear are the volume fraction φ of particles and the Péclet number $\mathrm{Pe} = 6\pi\eta a^3\gamma/kT$ measuring the relative importance of shear and hydrodynamic forces. $\mathrm{Pe}\to 0$ implies Brownian motion dominated behavior, while $\mathrm{Pe}\to\infty$ implies hydrodynamic dominated. Note that neither η_r^B nor η_r^I diverge as $\mathrm{Pe}\to 0$ as the scaling in Eq. (21) might indicate. As $\mathrm{Pe}\to 0$, $(1/N)\Sigma(\cdot)$ is $O(\mathrm{Pe})$ in both expressions so that the contributions to the stress are actually $O(1)$ as $\mathrm{Pe}\to 0$ (cf. the discussion by Batchelor[7]). Although we determine the complete bulk stress, we shall only discuss the viscosity here, normal stress differences will be discussed elsewhere.

We close this section by repeating here, for ease of reading, the evolution equation for particle positions formed from integrating the Langevin equation (see Bossis and Brady[4] for a complete discussion):

$$\begin{aligned}\Delta\mathbf{x} = \mathrm{Pe}\{\langle\mathbf{u}\rangle + \mathbf{R}_{FU}^{*-1}\cdot[\mathbf{R}_{FE}^{*}:\langle\mathbf{E}\rangle + \mathbf{F}^P]\}\Delta t \\ + \nabla\cdot\mathbf{R}_{FU}^{*-1}\Delta t + \mathbf{X}(\Delta t),\end{aligned} \tag{22}$$

$$\langle\mathbf{X}\rangle = O, \text{ and } \langle\mathbf{X}(\Delta t)\mathbf{X}(\Delta t)\rangle = 2\mathbf{R}_{FU}^{*-1}\Delta t,$$

where $\mathbf{X}$ is a random displacement.

III. SIMULATIONS RESULTS

We have discussed elsewhere,[4] the use of Stokesian dynamics with Brownian motion to determine particle motion. The only new point is the calculation of the Brownian stress $\mathbf{S}^B$ given by Eq. (11). We have performed simulations for a monolayer of identical spheres; in this case the convergence problems associated with the long-range hydrodynamics interaction are less important because the local rate of strain on a reference particle due to a stresslet located at a distance r decreases as $1/r^3$, and the integral over a monolayer is convergent. So, in principle, we have no long-range problem in the calculation of the viscosity. Nevertheless, if we assume a linear perturbation of the pair-distribution function $P_{1/1}(\mathbf{r})$ as a function of the Péclet number, which must be the correct asymptotic form as $\mathrm{Pe}\to 0$, we can write

$$P_{1/1}(\mathbf{r}) = ng(\mathbf{r}) = ng_0(\mathbf{r})[1 - (\mathrm{Pe}/2)f(r)(xy/r^2)], \tag{23}$$

and we can show by solving a two-sphere convection–diffusion equation for a monolayer[5] that the deformation function $f(r)$ decreases as $1/r$ at large distances. Thus one might fear that the use of periodic boundary conditions would perturb not only the long-range structure (which would not be critical for $1/r^3$ asymptotic behavior of the Brownian stress in a monolayer), but also the short-range behavior of $f(r)$. If the short-range structure were perturbed, the value of the Brownian or interparticle stress would depend on the size of the box. Similarly the hydrodynamic stress $\mathbf{S}^H$ contains a part coming from the velocities of the particles, which could also depend on the size of the unit cell. We have checked this cell dependency of the stress in two ways:

(1) First, we have used the Ewald summation with a replication of the planar unit cell on a cubic lattice so that the whole 3D system consists of equally spaced planes with a distance between the planes equal to the length of the unit cell. The hydrodynamic viscosity η_r^H has been calculated at zero Péclet number, because for a purely Brownian suspension, we can generate the configurations with a Monte Carlo hard-sphere simulation, which is very fast, and then calculate the average of S^H on uncorrelated configurations. The

Downloaded 13 Jan 2006 to 131.215.225.172. Redistribution subject to AIP license or copyright, see http://jcp.aip.org/jcp/copyright.jsp

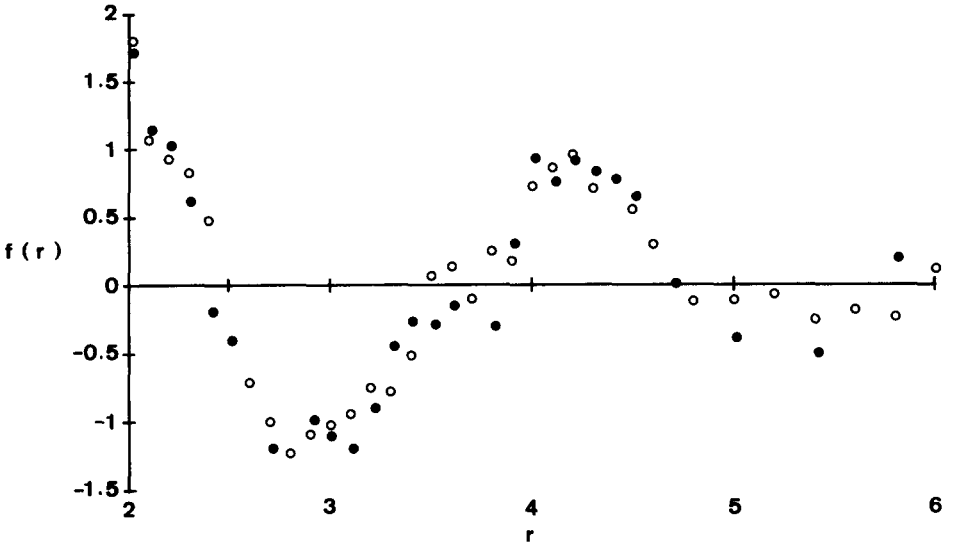

FIG. 1. Simulation results for the deformation function $f(r)$ for hard spheres defined in Eq. (23): (○) 49 particles (●) 25 particles.

hydrodynamic viscosity obtained for an area fraction $\varphi_A = 0.45$ with Ewald sums and 25 particles was: $(\eta_r^H)_{\mathrm{Ew}} = 0.77$ compared to $(\eta_r^H)_{PBC} = 0.72$ with periodic boundary conditions; for a higher density: $\varphi_A = 0.6$ we find $(\eta_r^H)_{\mathrm{Ew}} = 2.74$ and $(\eta_r^H)_{PBC} = 2.55$. This change ($\approx 7\%$), is very moderate and of no consequence for our analysis.

(2) Second, we have checked the deformation function $f(r)$ and the Brownian stress S^B for a Péclet number different from zero: (Pe = 0.5) with either 25 or 49 particles in the unit cell. The comparison is represented in Fig. 1. We can see that the deformation function $f(r)$ is the same, within uncertainty, in the region $2 < r < 5$. The precision is not sufficient to detect any long-range behavior, but in any case, this does not matter for the Brownian stress since we obtain 0.58 ± 0.05 for 25 particles and 0.53 ± 0.05 for 49 particles.

In brief the use of periodic boundary conditions does not seem to influence the determination of the stress for a monolayer. Furthermore, we are more interested in a study of the evolution of the viscosity with shear rate rather than in the absolute value of the viscosity of a monolayer.

The results for the viscosity as a function of the Péclet number are summarized in Table I and plotted in Fig. 2. We have used two kinds of systems at the same areal fraction: $\varphi_A = 0.453$. The first one is composed of hard spheres (there is no interparticle potential but the spheres do not overlap due to the hydrodynamic lubrication forces as discussed in Sec. II). This is a reference system and we shall discuss it in considerably more detail than the second system where we have added a soft interparticle repulsive force $\mathbf{F}^P = -\nabla V$ derived from a Debye–Huckel potential

$$V(r)/kT = Ce^{-\kappa(r-2)}/r. \tag{24}$$

We have chosen $C = 950$ and $\kappa = 12$ so that $F^P a/kT$ is of order one for Pe = 1 and a distance between two spheres corresponding to the formation of a square lattice.

The second and third column of the table give the number of steps and the time step either in units of a^2/D_0 for $\mathrm{Pe} \leqslant 1$ or in units of $1/\gamma$ for Pe > 1. For 25 particles a run of 30 000 time steps represents approximately one hour on a Cray 2. $\eta_r^H - (5/3)\varphi_A$ and η_r^B represent, respectively, the hydrodynamic viscosity coming for the shear flow (minus the self part which is 5/3 φ_A for a monolayer instead of

TABLE I. Results of the simulation of a monolayer of 25 identical hard spheres at an area fraction $\varphi_A = 0.453$ for different Péclet numbers. The second column is the number of steps of the run; the third column is the time step nondimensionalized by a^2/D_0 for Pe < 1 and by γ^{-1} for Pe > 1. The three following columns give the hydrodynamic (minus the self part), the Brownian, and the total relative viscosity of the hard-sphere suspension. The last column is the total relative viscosity of the spheres with a repulsive Debye–Huckel potential.

Pe	NSTEPS	Δt	$\eta_r^H - 5/3\,\varphi_A$	η_r^B	η_r^{HS}	η_r^{DH}
0	10 000		0.72 ± 0.01	0.91[a]	3.39	
0.25	90 000	10^{-3}	0.70 ± 0.01	0.80 ± 0.05	3.25	
0.375	60 000	10^{-3}	0.71	0.66 ± 0.05	3.12	2.99
0.5	30 000	2×10^{-3}	0.71	0.58 ± 0.05	3.04	
1	20 000	2×10^{-3}	0.72	0.50	2.97	
10	20 000	2×10^{-3}	1.04	0.185 ± 0.01	2.97	
10^2	25 000	2×10^{-3}	1.19	0.023	2.96	1.99
10^3	20 000	2×10^{-3}	1.27	2×10^{-3}	3.02	2.29
10^4	20 000	2×10^{-3}	1.51	1.6×10^{-4}	3.26	3.05
∞	20 000	2×10^{-3}	1.90	0	3.65	3.65

[a] Value estimated by extrapolation according to a quadratic scaling of the two lowest Pe values reported in the table.

Downloaded 13 Jan 2006 to 131.215.225.172. Redistribution subject to AIP license or copyright, see http://jcp.aip.org/jcp/copyright.jsp

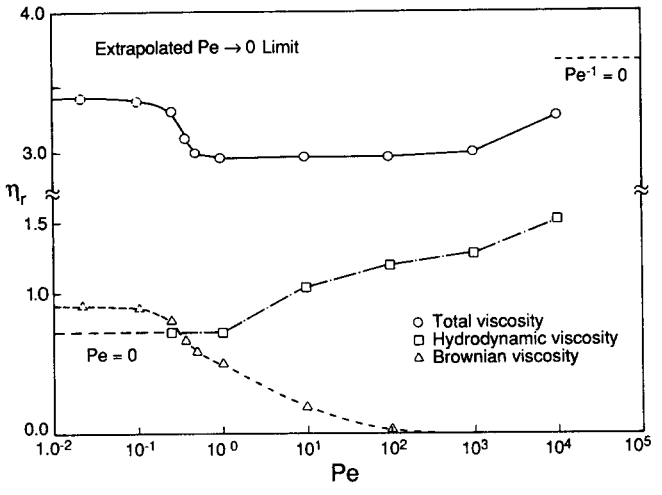

FIG. 2. Relative viscosity as a function of the Péclet number for a monolayer of hard spheres: (-O-) total relative viscosity; (--Δ--) Brownian contribution: η_r^B; (-□-) hydrodynamic contribution without the self part: $\eta_r^H - 5/3\,\varphi_A$.

Einstein's $5/2\,\varphi$) and the Brownian viscosity of this hard-sphere suspension. By hard-sphere suspension we mean a suspension of particles that interact uniquely through hydrodynamic and Brownian forces; there are no interparticle forces. We can see that the hydrodynamic part remains constant with a value of 0.71 ± 0.01 from $\mathrm{Pe} = 0$ to $\mathrm{Pe} = 1$ and then rises up to $\eta_r^H = 1.9$ for $\mathrm{Pe} = \infty$. It is worth noting that for $\mathrm{Pe} = 10^4$ even if the Brownian motion is very small (it scales as Pe^{-1}) its influence is still quite important since $\eta_r^H = 1.51$ instead of 1.9. The Brownian contribution at zero Péclet number has been extrapolated from a quadratic dependency on Péclet number: $\eta_r^B(\mathrm{Pe}) = \eta_r^B(0) - A\ \mathrm{Pe}^2$. General consideration about reversing the direction of shear in simple shear flow requires that the viscosity be a function of the square of the Péclet number.[22]

The total relative viscosity (η_r^{HS} in Table II) is presented in Fig. 2. The qualitative behavior is quite similar to that observed experimentally.[23–25] We observe a shear thinning region at low shear rates and then a plateau followed by a shear thickening region which begins between $\mathrm{Pe} = 10^3$ and $\mathrm{Pe} = 10^4$. This behavior can be easily understood by looking at the change in the local structure with the shear rate.

The Brownian viscosity is given by the relation (21c); and, as noted before, if we consider pairwise hydrodynamic interactions it reduces to

TABLE II. Cluster statistics as a function of the Péclet number. If the gap between two spheres is smaller than ϵ_C they belong to the same cluster. S_1 and S_2 are, respectively, the average size and average mass of the clusters [cf. Eqs. (26) and (27)].

P_e		$\epsilon_C = 10^{-3}$	$\epsilon_C = 10^{-2}$	$\epsilon_C = 10^{-1}$
0.25	S_1	1.006	1.025	1.305
	S_2	1.0115	1.052	1.671
100	S_1	1.054	1.372	2.34
	S_2	1.117	1.1936	5.25
∞	S_1	2.07	2.76	4.79
	S_2	5.17	7.67	13.06

$$\eta_r^B = -(27/16\pi)(\varphi^2/\mathrm{Pe}) \int W(r)xy/r^2 g(\mathbf{r})\,d\mathbf{r}, \quad (25)$$

where $W(r)$ is a known function of the separation distance $\mathbf{r}$ between the two spheres; at large distances (actually $r > 4a$) it decreases as $1/r^3$ for a monolayer[5] and $1/r^6$ for a 3D suspension,[7] whereas for two particles at contact $W = +6.96$ for a monolayer and $W = +6.37$ in 3D. At low Péclet numbers the deformation of the pair-distribution function is linear in the Péclet number as expressed by Eq. (23) and we get a constant value as $\mathrm{Pe} \to 0$. At higher shear rates the angular deformation of $g(\mathbf{r})$ no longer responds linearly, and appears to saturate at high Péclet numbers in the range $100 < \mathrm{Pe} < 10\,000$, as can be seen in Fig. 3 of Bossis and Brady.[4] On the other hand, the function $W(r)$ has no singularity for $r = 2a$ and decreases rapidly as a function of r. Thus we expect that the integral in Eq. (25) will become constant at high shear rates and that the viscosity will decrease as Pe^{-1} as the scaling in Eq. (25) indicates. This is indeed what we find numerically for $\mathrm{Pe} > 10$.

This apparent Pe^{-1} decay of the Brownian viscosity cannot, however be the ultimate scaling as $\mathrm{Pe} \to \infty$. The general considerations about reversing the direction of shear in simple shear flow, predict that the Brownian stress should ultimately decay as Pe^{-2} as $\mathrm{Pe} \to \infty$. That this should be the case can also be seen from Eq. (25) by noting that at $\mathrm{Pe}^{-1} = 0$, $g(\mathbf{r})$ is an even function of x (reversing the direction of flow does not change the structure), and thus the integral in Eq. (25) is zero. Perturbation from the infinite Péclet number state should proceed in inverse powers of Pe, i.e., $g(\mathbf{r}) \sim g_\infty(\mathbf{r}) + \mathrm{Pe}^{-1} g_{-1}(\mathbf{r}) + \ldots$ as $\mathrm{Pe} \to \infty$, and $g_{-1}(\mathbf{r})$ will be odd in x. Thus, the $\eta_r^B \sim \mathrm{Pe}^{-2}$ as $\mathrm{Pe} \to \infty$.

The simulation results shown in Table I are not, apparently, at high enough Péclet number to detect the proper scaling as $\mathrm{Pe} \to \infty$. The same can also be said of the low Péclet number results. The extreme limits of high and low Pe pose numerical difficulties as the deformation of the microstructure is slight, requiring a very high level of statistical accuracy.

The diminution of the Brownian viscosity with the Péclet number is responsible for the shear thinning behavior since the hydrodynamic part remains constant for $\mathrm{Pe} < 1$. The increase of the hydrodynamic viscosity accounts for the shear thickening part, and we shall see that it comes from the formation of transient clusters. In the absence of Brownian motion, experiments[26] and simulations[27] on a monolayer have demonstrated the existence of clusters whose size increases with the volume fraction of solids. These situations correspond to an infinite Péclet number. When Brownian motion is added, it efficiently destroys the larger clusters [principally through the action of $\nabla \cdot \mathbf{R}_{FU}^{-1}$ in Eq. (22)] as can be seen in Fig. 3 where we have plotted the percentage of spheres belonging to clusters which contain at least N spheres as a function of the size (in number of spheres) of each cluster. We see that for $\mathrm{Pe} = 0.25$ there are no clusters of three or more spheres, whereas for $\mathrm{Pe} = 10^4$, 40% of the spheres belong to clusters of 3 or more and at infinite Péclet number 68% belong to clusters of 3 or more. The large difference between the two curves for $\mathrm{Pe}^{-1} = 0$ and $\mathrm{Pe}^{-1} = 10^{-4}$ shows that a very small amount of Brownian

Downloaded 13 Jan 2006 to 131.215.225.172. Redistribution subject to AIP license or copyright, see http://jcp.aip.org/jcp/copyright.jsp

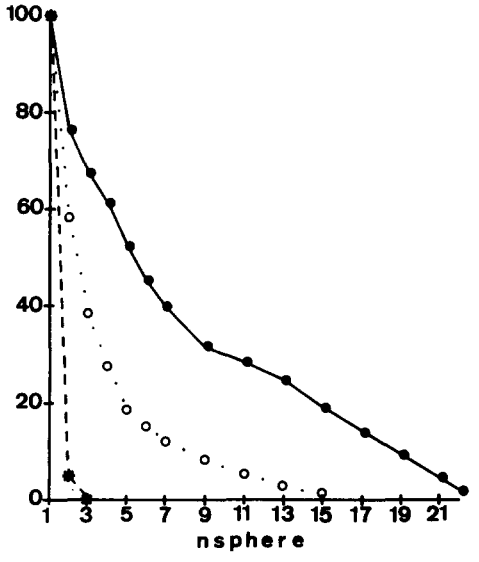

FIG. 3. Percentage of spheres belonging to clusters which contain at least N spheres: (-●-) $\mathrm{Pe}^{-1}=0$; (-○-) $\mathrm{Pe}=10^4$; (-*-) $\mathrm{Pe}=0.25$.

motion (10^{-4}) is still very efficient in breaking clusters. We have chosen 10^{-2} radii for the separation distance ϵ_C which defines that two spheres belong to the same cluster. This is quite reasonable since 10^{-2} also represents the characteristic range of the lubrication forces. In any event, changing the criterion to define a cluster does not change the qualitative behavior as can be seen from Table II where we have listed the number and the mass averaged moments of the cluster distribution, defined by

$$S_1=\Sigma_S S n_S/\Sigma_S n_S \tag{26}$$

and

$$S_2=\Sigma_S S^2 n_S/\Sigma_S S n_S, \tag{27}$$

where n_S is the number of clusters containing S particles. For each definition of the minimum separation ϵ_C we observe the same trend demonstrating the growth of cluster size with Péclet number.

This formation of clusters is clearly correlated with the increase of the hydrodynamic viscosity, but the relationship is not obvious at first sight. For a given volume fraction, if we form spherical clusters of radii a' such that $a'/a=(N/N')^{1/3}$ (where N and N' are, respectively, the number or particles of radius a and a' per unit volume), it amounts to rescaling all lengths by a' and the viscosity will be unchanged. (For a monolayer we have a 1/2 as opposed to a 1/3 power). In fact, there is some fluid imprisoned between the spheres inside the cluster and the new radius a' will be slightly larger than $a(N/N')^{1/3}$, which will contribute to increase the effective packing fraction and so the viscosity. For nonspherical clusters, however, the hydrodynamic stress is proportional to the cube of the larger dimension situated in the plane of shear; so, for the same number of particles per unit volume, elongated clusters will contribute much more to the viscosity than spherical ones. We have calculated a characteristic size L_C of the clusters by inscribing the centers of the particles in a rectangle and taking its diagonal. If we compare with the same quantity L_S calculated for a cluster of 4 spheres (square arrangement), and for 7 and 19 spheres (hexagonal packing) we get, respectively, the ratios $L_C/L_S=1.9$, 1.65, and 1.4, respectively, showing that, on average, the clusters are elongated and the elongation is more pronounced for the smaller ones. Furthermore, for a given number of spheres, this shape ratio is quite insensitive to the value of the Péclet number. These results clearly show that for hard-sphere suspensions the shear thickening is associated with the formation of elongated clusters, whereas the shear thinning is due to the nonlinear behavior of the Brownian stress coming directly from the nonlinear deformation of the local structure.

IV. DISCUSSION

Up to now shear thickening behavior has been observed for monodisperse systems in the presence of interparticle forces (often due to a stabilizing double layer). For coated silica spheres which exhibit a hard-sphere structure, no dilatant behavior has been observed by Van der Werff *et al.*,[3] but the maximum Péclet number ($\approx 10^2$) in these experiments is probably too low to observe the shear thickening predicted here, and there is a need for higher Péclet number measurements in order to see dilatancy in hard-spheres suspensions. (From Table I we see that $\mathrm{Pe}=10^4$ is needed before any shear thickening could be detected.)

The effect of a purely repulsive force on the rheology is given by the interparticle viscosity η_r^I, [cf. Eq. (21b)]. There is now a new parameter—the nondimensionalized force F^P and a detailed study of soft-sphere rheology is beyond the scope of this paper. Nevertheless, we have performed one simulation with the Debye–Huckel potential given by Eq. (24) for several different Péclet numbers in order to see if we recover the same qualitative behavior as for hard spheres. The results listed in the last column of Table I show that this is indeed the case with a minimum at $\mathrm{Pe}=10^2$ which is much deeper than for the hard-sphere potential. This behavior—a decrease of the viscosity at high Péclet numbers when the range of the repulsive force increases—has been experimentally observed.[25]

If we use pairwise hydrodynamics, Eq. (21b) for the interparticle viscosity reduces to the form

$$\eta_r^I=-(27/16\pi)(\varphi^2/\mathrm{Pe})\int r(1-A)f^p(r)xy/r^2 g(\mathbf{r})d\mathbf{r}, \tag{28}$$

where $f^p(r)$ is the nondimensional (by kT/a) interparticle force and A is the hydrodynamic function in (13). The form of η_r^I is very similar to that for η_r^B with pairwise hydrodynamics, Eq. (25); the only change needed is to replace $W(r)$ by $r(1-A)f^p(r)$. One should thus expect that the interparticle viscosity should behave in a manner analogous to the Brownian viscosity, provided that $r(1-A)f^p(r)$ is of the same general form as $W(r)$. At large separations [$r>\kappa^{-1}$ in Eq. (24)] f^p falls off rapidly as does $W(r)$. At short distances, however, the form of $f^p(r)$ will be important in determining the viscosity; $r(1-A)f^p(r)\approx 2(r-2)f^p(r)$ as $r\to 2$, and, provided $f^p(r)$ is less singular than $1/(r-2)$, η_r^I will behave as η_r^B. For the interparticle force used here this is the case; f^p reaches a large, but finite, value as $r\to 2$, and η_r^I

Downloaded 13 Jan 2006 to 131.215.225.172. Redistribution subject to AIP license or copyright, see http://jcp.aip.org/jcp/copyright.jsp

shear thins as Pe^{-1} in the large, but not infinite, Péclet number range. Again, as $\mathrm{Pe}\to\infty$ we should see an ultimate decay as Pe^{-2} from flow reversibility arguments.

Even if the repulsive interparticle force is singular as $r\to 2$, we can still estimate the asymptotic form of η_r^I for large Pe. Suppose that $f^p(r)\approx\xi^{-\alpha}$ as $\xi=r-2\to 0$, where $\alpha>0$. As the Péclet number increases, there will be a nearest neighbor peak in $g(\mathbf{r})$ formed on the upstream side of the reference particle, i.e., where the shear forces along the compressive axis balance the repulsive forces. This balance will occur when $\mathrm{Pe}=f^p(\xi)$; Pe represents the shear force normalized by kT/a. The peak in $g(\mathbf{r})$ will become very sharp and high, such that the dominant contribution to η_r^I in Eq. (28) will be from the region near maximum ξ_m of $g(\mathbf{r})$. Hence, in order of magnitude Eq. (28) becomes

$$\eta_r^I\approx(\varphi^2/\mathrm{Pe})\xi_m f^p(\xi_m). \tag{29}$$

But, $f^p(\xi_m)\approx\mathrm{Pe}$ from the balancing of shear and interparticle forces, and Eq. (29) becomes

$$\eta_r^I\approx\varphi^2\xi_m. \tag{29a}$$

Finally, assuming $f^p(\xi)\approx\xi^{-\alpha}$, we have $\xi_m\approx\mathrm{Pe}^{-(1/\alpha)}$, giving

$$\eta_r^I\approx\varphi^2\mathrm{Pe}^{-(1/\alpha)}. \tag{30}$$

Thus, regardless of the form of the repulsive interparticle force, it too shear thins, with an exponent depending on the nature of the singular form of the force near contact.

Since the interparticle viscosity vanishes in the limit $\mathrm{Pe}\to\infty$ and since the microstructure approaches that of a hard-sphere system, we should always see an ultimate shear thickening of the suspension owing to the formation of elongated clusters. The effect of a repulsive interparticle force on cluster size is very similar to that of Brownian motion shown in Fig. 2 and Table II. The precise value of the Péclet number or dimensionless shear rate will, of course, depend on the particular interparticle force, but the qualitative trends remain the same. The effect of the repulsive interparticle force is to delay the formation of the clusters and so the onset of shear thickening but dilatancy should always be observed due to the increase of η_r^H, with the viscosity reaching a constant asymptote as $\mathrm{Pe}\to\infty$.

Experimental studies of suspensions do not seem to verify this predicted "hydrodynamic" dilatancy. In Brownian suspensions with repulsive interparticle forces,[24] there has been observed a shear thinning region, followed by shear thickening, followed by a further region of shear thinning, but no ultimate shear thickening. Two separate regions of shear thinning can be explained by the fact that both the Brownian and interparticle force contributions to the bulk stress shear thin, and the juxtaposition in dimensionless shear rate where these two shear thinning mechanisms occur can produce either one or two regions of shear thinning. The proper juxtaposition depends, of course, on the detailed form of the interparticle force and no general statements can be made.

The lack of any observations of an ultimate shear thickening behavior as the shear rate increases could be due simply to the fact that large enough shear rates (or Péclet number) have not been investigated experimentally. In the Brownian suspensions studied here, a Péclet number in excess of 10^4 is needed in order to observe the shear thickening, and with the Debye–Huckel repulsive potential an even higher shear rate is needed. There may be other explanations, however, that mask the ultimate shear thickening behavior, such as the formation of plug flow regions at high concentrations and shear rates, precluding the treatment of the suspension as a homogeneously sheared material. The sensitivity of the hydrodynamic viscosity to cluster formation (the cluster size increases with increasing volume fraction[27]) makes the viscosity particularly sensitive to edge and boundary effects during an experiment. Further, well defined and controlled experiments with the simultaneous measurement of viscosity and microstructure are needed in order to answer some of these intriguing questions.

APPENDIX

Stresslet due to Brownian motion

According to Eq. (11), the Brownian stresslet is defined by

$$\mathbf{S}^B=-(1/\Delta t)\int_0^{\Delta t}\mathbf{R}_{SU}^*(t)\mathbf{U}^B(\mathbf{t})\mathbf{dt}. \tag{A1}$$

During a time Δt the Brownian velocity $\mathbf{U}^B(t)$ will give a random displacement that is characterized by its two first moments:

$$\langle\Delta\mathbf{X}^R\rangle=O \text{ and } \langle\Delta\mathbf{X}^R\Delta\mathbf{X}^R\rangle=2\mathbf{D}\Delta t,$$

and a convective displacement: $\Delta\mathbf{X}^C=\nabla\cdot\mathbf{D}\Delta t$, where $\mathbf{X}$ is the $6N$ displacement (rotation-translation) vector and $\mathbf{D}=kT\mathbf{R}_{FU}^{-1}$ is the $6N\times 6N$ diffusion tensor. These Brownian displacements can be obtained from the N-particle Fokker–Planck or Smoluchowski equation for the distribution function $P_N(\mathbf{r}_1\ldots\mathbf{r}_N)$:

$$(\partial P_N/\partial t)=-\nabla\cdot[P_N\mathbf{V}-\mathbf{D}\cdot\nabla\mathbf{P}_N], \tag{A2}$$

where $\mathbf{V}$ is the $6N$ velocity vector coming from the external flow or interparticle forces.

According to Lax[28] and Zwanzig[29] the corresponding Langevin-type equation for the total velocities of the particles can be written as [note that there is a sign error in the Eq. (23) of Ref. 31]:

$$(d\mathbf{X}/dt)=\mathbf{V}+\boldsymbol{\sigma}\cdot\nabla\cdot\boldsymbol{\sigma}+\boldsymbol{\sigma}\cdot\mathbf{f}^R=\mathbf{V}+\mathbf{U}^B, \tag{A3}$$

where $\boldsymbol{\sigma}$ is the square root of the diffusion tensor, $\mathbf{D}=\boldsymbol{\sigma}\cdot\boldsymbol{\sigma}^+$, and $\mathbf{f}^R$ a $6N$ random force which satisfies:

$$\langle\mathbf{f}_p^R(t)\mathbf{f}_q^R(s)\rangle=2\delta_{pq}\delta(t-s), \tag{A4}$$
$$\langle\mathbf{f}^R\rangle=0.$$

With the expression (A3) for the Brownian velocity (A1) becomes:

$$\mathbf{S}^B=-\frac{1}{\Delta t}\int_0^{\Delta t}\{\mathbf{R}_{SU}\cdot\boldsymbol{\sigma}\cdot\nabla\cdot\boldsymbol{\sigma}+\mathbf{R}_{SU}\cdot\boldsymbol{\sigma}\cdot\mathbf{f}^R\}dt. \tag{A5}$$

The quantities $\mathbf{R}_{SU}\cdot\boldsymbol{\sigma}\cdot\nabla\cdot\boldsymbol{\sigma}$ and $\mathbf{R}_{SU}\cdot\boldsymbol{\sigma}$ depend on time, through the change of the positions of the particles in time. To evaluate Eq. (A5) we use a first-order development for a quantity $A(t)$:

$$A[\mathbf{X}(t)]=A[\mathbf{X}(0)]+(\nabla A)\cdot d\mathbf{X}(t),$$

with from Eq. (A3):

Downloaded 13 Jan 2006 to 131.215.225.172. Redistribution subject to AIP license or copyright, see http://jcp.aip.org/jcp/copyright.jsp

$$d\mathbf{X}(t) = (\mathbf{V} + \boldsymbol{\sigma}\cdot\nabla\cdot\boldsymbol{\sigma})t + \boldsymbol{\sigma}(o)\cdot\int_0^t \mathbf{f}^R(s)ds.$$

Thus we have

$$\frac{1}{\Delta t}\int_0^{\Delta t} \mathbf{R}_{SU}\cdot\boldsymbol{\sigma}\cdot\nabla\cdot\boldsymbol{\sigma}\mathbf{dt} = \mathbf{R}_{SU}\cdot\boldsymbol{\sigma}\cdot\nabla\cdot\boldsymbol{\sigma} + \mathbf{O}(\Delta t^2), \quad (A6)$$

$$\frac{1}{\Delta t}\int_0^{\Delta t} \mathbf{R}_{SU}\cdot\boldsymbol{\sigma}\cdot\mathbf{f}^R dt = \frac{1}{\Delta t}\nabla_p(R^{SU}_{ijk}\cdot\sigma_{km})\sigma_{pq}\int_0^{\Delta t} dt \times \int_0^t f^R_q(t)f^R_m(s)ds + 0(\Delta t^2),$$

or using:

$$\frac{1}{\Delta t}\int_0^{\Delta t} dt f^R_q(t)f^R_m(s) = \langle f^R_q(t)f^R_m(s)\rangle = 2\delta_{qm}\delta(t-s),$$

$$\frac{1}{\Delta t}\int_0^{\Delta t} \mathbf{R}_{SU}\cdot\boldsymbol{\sigma}\cdot\mathbf{f}^R dt = \nabla_p(R^{SU}_{ijk}\cdot\sigma_{km})\sigma_{pm}. \quad (A7)$$

Putting Eqs. (A6) and (A7) into Eq. (A5) we get for the Brownian stress:

$$S^B_{ij} = -\langle\partial_p(R^{SU}_{ijk}\sigma_{km}\sigma_{pm})\rangle,$$

or since $\mathbf{D} = \boldsymbol{\sigma}\cdot\boldsymbol{\sigma}^+ = kT\mathbf{R}^{-1}_{FU}$,

$$S^B_{ij} = -kT\partial_p(R^{SU}_{ijk}R^{-1}_{kp})(i,j,k,p = 1,...6N), \quad (A8)$$

which is Eq. (11).

[1]J. F. Brady and G. Bossis, Annu. Rev. Fluid Mech. **20**, 111 (1988).
[2]R. J. Phillips, J. F. Brady, and G. Bossis, Phys. Fluids **31**, 3462 (1988).
[3]J. C. Van der Werff, C. G. de Kruif, C. Blom, and J. Mellema, Phys. Rev. A **39**, 795 (1989).
[4]G. Bossis and J. F. Brady, J. Chem. Phys. **87**, 5437 (1987).
[5]G. Bossis, J. F. Brady, and C. Mathis, J. Colloid Interface Sci. **126**, 1 (1988).
[6]G. K. Batchelor, J. Fluid Mech. **41**, 419 (1970).
[7]G. K. Batchelor, J. Fluid Mech. **83**, 97 (1977).
[8]W. B. Russel and A. P. Gast, J. Chem. Phys. **84**, 1815 (1986).
[9]G. K. Batchelor and J. T. Green, J. Fluid Mech. **56**, 401 (1972).
[10]D. Bedeaux, J. Colloid Interface Sci. **118**, 80 (1987).
[11]R. W. O'Brien, J. Fluid Mech. **91**, 17 (1979).
[12]C. W. J. Beenakker, J. Chem. Phys. **85**, 1581 (1986).
[13]J. F. Brady, R. J. Phillips, J. C. Lester, and G. Bossis, J. Fluid Mech. **195**, 257 (1988).
[14]D. L. Ermak and J. A. McCammon, J. Chem. Phys. **69**, 1352 (1978).
[15]For a derivation note that the time rate of change in orientation $d\mathbf{p}/dt = \boldsymbol{\Omega}\cdot\mathbf{p} + \beta[\mathbf{E}\cdot\mathbf{p} - \mathbf{p}(\mathbf{p}\cdot\mathbf{E}\cdot\mathbf{p})]$ where $\beta = (r^2-1)/(r^2+1)$ is a function of the aspect ratio r of the particle and $\boldsymbol{\Omega}$ is the vorticity tensor.
[16]J. G. Kirkwood and P. L. Auer, J. Chem. Phys. **19**, 281 (1951).
[17]H. Giesekus, Rheol Acta **2**, 50 (1962).
[18]E. J. Hinch and L. G. Leal, J. Fluid Mech. **52**, 683 (1972).
[19]L. G. Leal and E. J. Hinch, J. Fluid Mech. **55**, 745 (1972).
[20]H. Brenner, Int. J. Multiphase Flow **1**, 195 (1974).
[21]Note also that Eq. (29) in Russel and Gast (Ref. 8) is incomplete as they have neglected an $O(\mathrm{Pe})$ contribution due to the deformation of the potential of mean force with shear (cf. discussion in Ref. 5). The errors in Ref. 8 have recently been corrected in N. J. Wagner and W. B. Russel, Physica A **155**, 475 (1989).
[22]See, for example, R. B. Bird, R. C. Armstrong, and O. Hassager, *Dynamics of Polymeric Liquids* (Wiley, New York, 1977), Vol. 1, p. 141, as well as Ref. 18–20.
[23]I. M. Krieger, Adv. Colloid Interface Sci. **3**, 111 (1972).
[24]R. L. Hoffman, Adv. Colloid Interface Sci. **17**, 161 (1982).
[25]H. M. Laun, Angew. Makromol. Chem. **123**, 335 (1984).
[26]C. Camoin, R. Faure, R. Blanc, and J. F. Roussel, Europhys. Lett. **3**, 419 (1987).
[27]J. F. Brady and G. Bossis, J. Fluid Mech. **155**, 105 (1985).
[28]M. Lax, Rev. Mod. Phys. **38**, 541 (1966).
[29]R. Zwanzig, Adv. Chem. Phys. **15**, 325 (1969).

Downloaded 13 Jan 2006 to 131.215.225.172. Redistribution subject to AIP license or copyright, see http://jcp.aip.org/jcp/copyright.jsp